Polym. Bull. (2012) 68:2033–2047
DOI 10.1007/s00289-012-0714-1

ORIGINAL PAPER

Complete relaxation map of polypropylene: radiation-induced modification as dielectric probe

E. Suljovrujic

Received: 29 December 2011 / Accepted: 29 January 2012 / Published online: 3 February 2012

Abstract The molecular relaxation behaviour of isotactic polypropylene (iPP) exposed to gamma radiation in air to various absorbed doses (up to 700 kGy) has been investigated by dielectric loss (tan δ) analysis; the polar (mainly carbonyl and hydroperoxide) groups that were introduced by radiation-induced oxidation were considered as tracer groups. All relaxation zones (α, β, γ and δ in the order of decreasing temperature), between 25 K and melting temperature, were studied in the frequency range from 1 kHz to 1 MHz. The changes observed in the dielectric relaxation spectra were related to the modifications in the structural and morphological parameters attributed to exposure of the iPP samples to radiation. Wide-angle X-ray diffraction was used to investigate radiation-induced changes in the crystalline structure and degree of crystallinity, since the α relaxation is connected with this phase. Infrared spectroscopy and gel measurements were used to determine the changes in the oxidative degradation and the degree of network formation, respectively. Conclusions derived using different methods were compared. This study reveals high dielectric and/or relaxation sensitivity of iPP to gamma radiation. Disappearance of the low-temperature dielectric (γ and δ) relaxations together with large changes in intensity, position and activation energy of the dielectric α relaxation are observed with gamma irradiation and are mainly connected with oxidative degradation in iPP structure.

Keywords Polypropylene · Gamma radiation · Oxidation · Dielectric relaxation · Polar groups

Introduction

Polypropylene (PP) belongs to the family of polyolefins. It has excellent mechanical and dielectric properties and therefore a wide variety of industrial applications,

E. Suljovrujic (✉)
Vinca Institute of Nuclear Sciences, University of Belgrade, Belgrade, Serbia
e-mail: edin@vinca.rs

including electrical ones. Due to the low-dielectric loss and good heat resistance, it has been widely used as electrical insulation, e.g. for cables and as a dielectric in power capacitors [1–3]. The measurable dielectric relaxations and losses in apolar PP are generally ascribed to impurities and to the fact that it is always slightly oxidized and thus contains polar carbonyl, peroxy or hydroperoxy groups. Among impurities, residual catalysts and antioxidants have been reported to affect the dielectric properties [4]. However, for the electrical application of such polymers, it is of essential interest to understand the dielectric phenomena in them. Dielectric measurements can also give valuable information about the structure and dynamics of materials [5]. In relaxation studies, PP displays four mechanical/dielectric relaxations, designated as α, β, γ and δ in the order of decreasing temperature, in addition to the melting point [4–24]. The origins of these relaxations have been studied in the past, mainly by mechanical measurements. However, a few dielectric studies are also available [4, 9–11]. Although some detailed molecular assignments are still open to debate, the reality of the basic relaxation processes is clear. The α and β relaxations are undoubtedly connected with the crystalline and amorphous phases, respectively. According to Jourdan et al. [7], the α relaxation is due to a relaxation of defects in the crystalline phase, but the amorphous phase in the neighbourhood of the crystallites also contributes to this process. This relaxation has a multiple nature, consisting of two or even more processes in the α relaxation zone [6, 17, 18]. The β relaxation is attributed to the glass–rubber transition in the amorphous phase of isotactic PP (iPP) [7]. According to different authors, the γ relaxation is due to the localized (most probably crank-shaft type) motions of either chain ends or branches associated with the amorphous phase [11, 18, 20], although originally it was also proposed to arise from the crystalline phase. In dielectric relaxation measurements, iPP may also exhibit a fourth relaxation, mainly below 100 K, which is named the δ process; this relaxation is weak or absent and is attributed to the hindered rotation of CH_3 groups [8, 10].

In order to better investigate the molecular relaxations, different structural and morphological modifications have been performed in the past, mainly by drawing, thermal treatment, irradiation, ageing, slight oxidation of the chains and by doping the polymer matrix with polar molecules and particles as probes. In general, radiation-induced structure modifications can be exploited not only from the standpoint of commercial applications but also as a useful tool for highlighting some of the fundamental processes and properties of polymers. Thus, exposition to radiation can be used to increase the dielectric activity and to investigate low-visible dielectric relaxations in apolar polyolefins [19, 25]. Even though the overall radiation chemistry of PP was investigated in detail and several comprehensive reviews are available on this topic [26–31], the effects of radiation on dielectric relaxation behaviour have not been investigated to an appreciable extent [6, 19, 21, 32–34]. A major application of high-energy radiation is cross-linking of insulation; cross-linking to a gel content of 55% was shown to be beneficial for cable insulation [26]. By linking the macromolecules into a network, the toughness, impact resistance, chemical resistance and working temperatures are improved [35]. A second major application of high-energy radiation is sterilization of the medical disposables. Furthermore, polyolefins are also used in many applications (nuclear

power plants, radiation equipment, sterilization systems, space-based applications, etc.) where exposure to high-energy radiation can occur. Radiation-induced changes greatly influence the dielectric properties (electric strength, dielectric loss, permittivity, electric conductivity, charge state, etc.) and dielectric relaxation spectra of apolar polymers such as iPP. The introduction of carbonyl, hydroperoxide and other polar groups as a result of radiation-induced oxidation intensifies dielectric losses. Furthermore, cross-linking and chain scission affect the mobility of macromolecules, especially in the amorphous phase, causing a shift of the relaxation maxima and a change in activation energy of dielectric relaxation to which the mentioned dipolar and molecular movements contribute [36].

Our aim is to draw a complete dielectric relaxation map of virgin and gamma-irradiated iPP and to establish a connection between the evolution of the dielectric relaxations and the radiation-induced changes in the structure. Dielectric relaxation spectroscopy (DRS) and gamma radiation were used as powerful methods for characterization and modification of polymer structure, respectively. In the case of dielectric relaxation measurements, the polar groups that were introduced by radiation-induced oxidation in apolar iPP were considered as tracer groups whose motion reflects the motion of polymer chains. A variety of supplementary measurements were made to qualitatively determine the radiation-induced changes in the structure. The results obtained by infrared (IR), WAXS and gel measurements were compared with the changes in the intensity, position and activation energy of dielectric relaxations.

Experimental

The polymer used in this study was a stabilized iPP, HIPOL MA2CR type C-7608 ($M_w = 136000$, $M_w/M_n = 4.95$, $\rho = 0.906$ g cm^{-3}). Isotropic sheets were prepared by 20 min compression moulding in a Carver laboratory press at 190 °C and gradual increment pressure up to 3.28 MPa. The moulded sheets were quenched in an ice–water mixture. The samples were wrapped in Al-foil and irradiated in a ^{60}Co radiation facility, in air, at room temperature, at a dose rate of 9 kGy/h, to various absorbed doses up to 700 kGy. Furthermore, it should be emphasised that the irradiated samples were annealed (at 95 °C) for 3 h in air, in order to minimize post-irradiation oxidation. The annealed irradiated samples, all 0.28 ± 0.02 mm thick, were used for further investigations.

Wide-angle X-ray diffractograms (WAXD) of the samples were obtained using a Bruker D8 Advance Diffractometer (in normal mode, with Cu Kα emission). The parallel beam optics was adjusted by a parabolic Göbel mirror (push plug Ni/C) with horizontal grazing incidence soller slit of 0.12° and LiF monochromator; diffractometer scans were taken in the angular range of $2\theta = 10°$–45°, at a step of 0.02°, with 10 s exposition per step. Furthermore, crystallinity was evaluated from diffraction curves by resolving multiple peak data into individual crystalline peaks and an amorphous halo. Quantitative analysis and fitting of multiple peaks in experimental spectra were performed using standard software with asymmetric pseudo-Voigt functions. For the gel measurements, the samples were inserted into a

200 mesh stainless steel cloth and immersed in xylene with 0.5 wt% antioxidant (Irganox 1010). The gel content was determined by the measurement of weight loss of the samples after solvent extraction in the boiling xylene for 17 h, followed by drying the samples for 4 h in a vacuum oven at 60 °C. The results are average values of five identically prepared samples. Furthermore, sol–gel calculations are based on the Charlesby–Pinner (C–P) expressions. A Carl-Zeiss Model 75IR Specord was used for recording IR spectra. The absorbance at 1,715 cm^{-1} was determined from these spectra. The oxidative (carbonyl) content was measured through normalized absorbance (A/d values; A = absorbance; d = sample thickness) at 1,715 cm^{-1}. The dielectric loss tangent (tan δ) of the samples in the form of discs 1.3 cm in diameter was measured on a Digital LCR Meter 4284A coupled with a 22C-kriodin(R) cryosystem, as a function of temperature (25–405 K) and in the frequency range 1 kHz to 1 MHz. Dielectric measurements were taken at increments of approximately 2 K during a heating run from 25 to 405 K, with the heating rate of 1.7 K min^{-1} between equilibrated temperatures. At each equilibrated temperature, measurements of capacitance and tan δ were taken at several frequencies from 1 kHz to 1 MHz; data acquisition over the frequency range required about 5 min.

Results and discussion

Dielectric relaxation spectra for virgin iPP presented in Fig. 1a confirm the presence of all four relaxations; at a frequency of 100 kHz, the high-temperature α relaxation, glass transition, i.e. β relaxation, and two low-temperature (γ and δ) relaxations can be observed around 330, 300, 220 and 100 K, respectively. The α and β relaxation transitions are seen as prominent loss peaks, while the low-temperature γ and δ transitions are less visible. The β process is well resolved from the γ relaxation at moderate frequencies (Fig. 1a). However, this is not true with respect to the dielectric α process. The α process occurs at a higher temperature than the β, but its activation energy is lower. This means that the α and β processes become better resolved in isochronal scans as frequency increases. Furthermore, while the magnitude of the β process decreases with frequency, the magnitude of the α process shows opposite behaviour. At higher frequencies (1 MHz), multiple nature of the dielectric α process is clearly evident (Fig. 1a). It was found by Pluta and Kryszewski that the morphology and structure differentiation significantly influence the nature and the number of components of the mechanical α relaxation process [18]. The presence of a smectic phase as well as the decrease of both the spherulite size and the structure perfection lead to enhancement of the mobility of crystallites, and consequently to an increase of the contribution from the intralamellar regions to the α relaxation process. Two clearly evident components of the mechanical α relaxation process were found for nonspherulitic samples, crystallized from the glassy state. The low-temperature component is mainly attributed to the stress relaxation of the fraction of the noncrystalline phase containing strained molecules and segments of molecules belonging to the specific (irregular) arrangement of the surface layer of the crystallites. The high-temperature component of the α relaxation

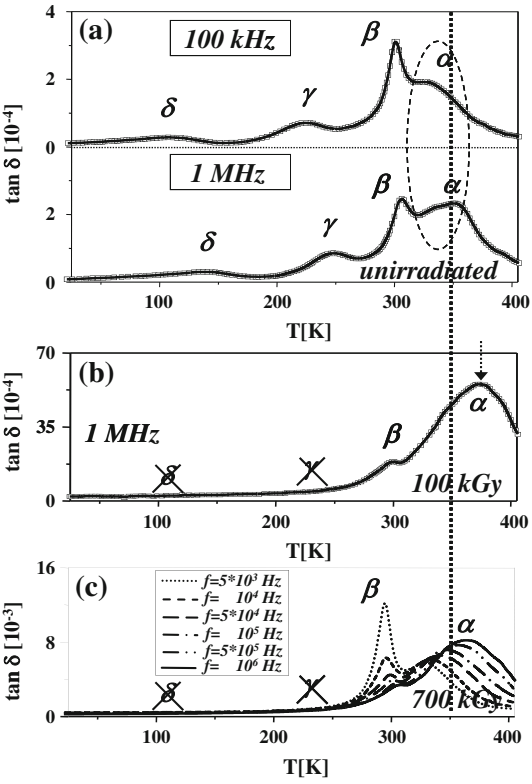

Fig. 1 **a** Dielectric loss tangent versus temperature for virgin iPP sample at two different frequencies (100 kHz and 1 MHz); **b** dielectric loss tangent versus temperature, at $f = 1$ MHz, for iPP sample irradiated in air to 100 kGy; **c** dielectric loss tangent versus temperature, at several frequencies from 5 kHz to 1 MHz, for iPP sample irradiated in air to 700 kGy

process is connected with the viscous slip process of the crystalline elements within the noncrystalline phase. The intensity of this process increases with the decrease of crystallite size. The presence of the smectic phase in the nonspherulitic structure enhances the extent of that process. Furthermore, an impressive study of the mechanical α relaxation as a two-component process was made by Tiemblo and collaborators for the case of iPP exposed to thermo-oxidation [16, 17]; they proposed that the α relaxation makes it possible for crystals to act as radical scavengers and thus stabilize iPP exposed to thermo-oxidation at temperatures under 115 °C. On the other hand, the dielectric α relaxation is almost unexplored [6]. Actually, very few experimental results are available, and most of them are made by TSDC measurements applied to investigate charge traps in crystalline parts [37, 38]. Comparison with the α relaxation in PE was made, too [39]. Mansfield and Boyd have proposed that the dielectric α process in PE can be represented by the propagation process of α twisted defect along the chain within crystal lattice, leading to reorganization of the crystal surface [40]. On the other hand, the mechanically active α process in PE, although it requires the presence of the crystal phase, has the relaxation strength assigned to the amorphous component and involves softening or deformation of the latter. However, in the case of PP, the relaxation times for the α process follow the Arrhenius law due to less cooperative motions than in the case of the glass rubber transition, i.e. β relaxation. Activation

energies for this process usually range from 90 to 170 kJ mol^{-1} [7, 22], but much higher values (up to 350 kJ mol^{-1}) are also reported [4]. The intermediate β peak situated around 300 K has been attributed to the glass transition of the amorphous phase. Due to the broadness of this relaxation, some authors proposed two transitions involving unconstrained regions of the amorphous phase and regions constrained by crystallites (which may depend on the crystallite size [22]) [4, 7]. The Vogel–Fulcher–Tammann (VTF) or its equivalent, the Williams–Landel–Ferry temperature dependence observed for this relaxation indicates cooperative behaviour related to the glass transition [41–43]. Despite this, the Arrhenius temperature dependence is also widely used [7, 12, 22, 44, 45]. The reported apparent activation energies are in the range of 300–690 kJ mol^{-1} [7, 12, 22, 41–45]. The low-temperature dielectric γ and δ processes, observed around 220 and 100 K, are usually assigned to the local (most probably crank-shaft type) motions in the amorphous phase [11, 18, 20] and to the hindered rotation of CH_3 groups [8, 10], respectively. An Arrhenius temperature dependence is observed for low-temperature relaxations and reported activation energies for the γ and δ relaxations are about 25 and 5 kJ mol^{-1}, respectively [10]. Objective values for the temperatures of the relaxation processes were obtained using curve fitting from isochronal loss scans at several frequencies (isochronal loss scans at 100 kHz and 1 MHz are shown in Fig. 1a). Loss map for the dielectric processes is presented in Fig. 2a. The α, γ and δ processes show Arrhenius behaviour

$$f_{\max} = f_{\max,\infty} \exp\left(-\frac{E_a}{kT}\right) \tag{1}$$

where $f_{\max,\infty}$ is a dimensional parameter, E_a is the activation energy and k is Boltzmann's constant. Apparent activation energies for the dielectric α, γ and δ relaxations are 115, 35 and 7 kJ mol^{-1}, respectively, and are in good agreement with the literature data. On the other hand, the Arrhenius plot of the β relaxation is significantly bent, which indicates cooperative behaviour. This is a typical feature found with relaxations that are related to glass transition. It confirms the hypothesis that the β relaxation in iPP is related to the glass transition in the amorphous phase. The $f_{\max}(T)$ function of the β relaxation is fitted by the VFT–Hesse (VFTH) equation:

$$f_{\max} = f_{\max,\infty} \exp\left(-\frac{B}{T - T_\infty}\right) \tag{2}$$

where $f_{\max,\infty}$, B and the Vogel temperature T_∞ are VTF parameters [46]. The Vogel temperature is closely related to the dynamic glass-transition temperature T_g, which is usually defined as the temperature where the relaxation time is $\tau = 100$ s. The VTF parameters are also used for determining the dynamic fragility m and the apparent activation energy E_a at T_g [43]; the values of the calculated parameters are given in Table 1. For virgin iPP, the values obtained for the glass-transition temperature $T_g = 281$ K, dynamic fragility $m = 103$ and apparent activation energy at glass-transition $E_g = E_a\ (T_g) = 560$ kJ mol^{-1} are in good agreement with the results published by Plazek and Ngai [47].

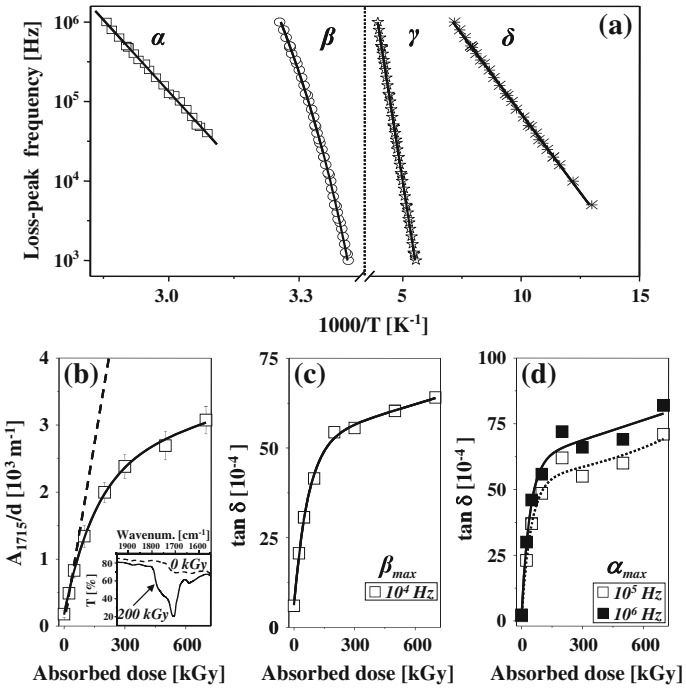

Fig. 2 **a** Loss map for the α, β, γ and δ processes in virgin iPP. The full curves are Arrhenius fits to the dielectric α, γ and δ relaxations as well as VFTH fit to the dielectric β relaxation. The correlation factor of the fits is equal to or better than $r = 0.995$. The calculated parameters are given in the text and in Table 1; **b** normalized IR absorption intensity (A/d values; A = absorbance; d = sample thickness) at 1,715 cm^{-1} versus absorbed dose. Shown by the *inset* are the IR spectra in the carbonyl region for virgin and irradiated (200 kGy) iPP samples; **c** the intensity of the dielectric β relaxation as a function of absorbed dose measured at 10 kHz; **d** the intensity of the dielectric α relaxation as a function of absorbed dose measured at two different frequencies: 100 kHz and 1 MHz

Table 1 The values of the glass-transition temperature T_g, dynamic fragility m and apparent activation energy at glass-transition $E_g = E_a(T_g)$ obtained using the VFTH equation on the dielectric β relaxation in virgin and irradiated iPP

Parameters obtained by using the VFTH equation	Absorbed dose							
	0	25	50	100	200	300	500	700
$T_g = T_\beta$ (τ = 100 s) (K)	281.3	279.7	278.9	277.1	276.7	279.5	281.9	281.5
m	102.9	100.1	95.9	92.2	92.0	98.6	105.2	103.7
$E_g = E_a$ (T_g) (kJ mol^{-1})	557.2	538.8	514.6	491.6	489.9	530.6	571.1	561.9

By comparing the dielectric loss scans, for the virgin and irradiated samples (Fig. 1), it can be observed that the radiation qualitatively changes the dielectric γ and δ relaxation zones and introduces significant quantitative changes in the dielectric α and β relaxation zones. The disappearance of the already weak low-temperature dielectric γ and δ relaxations with gamma radiation is evident.

The γ relaxation has practically "vanished" with gamma irradiation in air, as in the case of ultraviolet rays [14]. The dynamic mechanical investigation of iPP thermo-oxidative degradation has indicated that the initiation of thermal oxidation is concomitant with a partial vanishing of the γ relaxation, too [16, 17, 20]. In general, it looks that oxidative degradation of iPP structure plays critical role in the disappearance of the low-temperature dielectric relaxations. On the other hand, the radiation-induced changes in the dielectric α and β relaxations are emphasised. Changes in the intensity of dielectric β and α relaxations with gamma irradiation are related to radiation-induced oxidation. The radiation-induced increase in the amount of carbonyl, hydroperoxide and other polar groups in apolar iPP causes modification of the dielectric properties due to the increase in polymer polarity [19, 33, 34, 48–50]. Moreover, it is known that polar groups generate shallow traps and enhance charge injection [5, 51, 52]. It is very difficult, almost impossible, to detect from dielectric measurements the presence of specific polar groups, but all together they will give contribution to dielectric behaviour [53].

Exposure of iPP films to radiation in air results in a significant increase in oxidation and the formation of hydroperoxides and/or carbonyls as major products [54]. The mechanism commonly invoked in the radiation-induced oxidation process of PP is the attack of free radicals on the polymer chains. The alkyl radicals generated in this way react with oxygen, giving rise to hydroperoxides, alcohols, and carbonyl compounds such as carboxylic acids, ketones and esters, whose relative percentage depends on oxidation conditions [55, 56]. The quantification of the various oxidation products of PP (as a result of gamma, photo, and thermal oxidation) was done by Lacoste et al. [57, 58]. The radiation-induced modifications that occur in the hydroxyl and carbonyl region were investigated in our previous papers [6, 21, 32], too. The major oxidation products in irradiated iPP are the tertiary hydroperoxides, which are unstable and undergo radical decomposition to other more stable oxidative products with an increase in radiation dose and their concentration. This is a major source of carbonyl compounds, especially at higher radiation doses. In the carbonyl region, the increase of absorbance in the range 1,725–1,715 cm^{-1} indicates the formation of ketones (inset in Fig. 2b). Saturated carboxylic acids are generally observed at 1,755 and 1,718–1,710 cm^{-1}, while unsaturated acids absorb around 1,700 cm^{-1}. The absorptions around 1780, 1740 and 1725 cm^{-1} are usually ascribed to lactones, esters and aldehydes, respectively [54]. Ketones and carboxylic acids, responsible for the absorption maxima at 1,715 cm^{-1}, are the main radiation-induced oxidation products observed in the carbonyl region. The evolution of carbonyl content (through the normalized absorbance at 1,715 cm^{-1}) with absorbed dose is presented in Fig. 2b. A linear dependence of the carbonyl content is evident for lower doses, while for higher ones (>200 kGy) an intense deviation (saturation) from linear curve occurs. The saturation in the carbonyl content for the iPP samples irradiated in air coincides with the start of gelation (Fig. 3b). Gavrila and Gosse [59] have also found for the iPP gamma-irradiated in air that the amount of carbonyl groups declines sharply at the gel point. However, the generation of oxidizing species can probably be suppressed by intensive cross-linking behaviour and the formation of net structure, but more probably the real reason for the saturation in carbonyl and hydroperoxide contents is

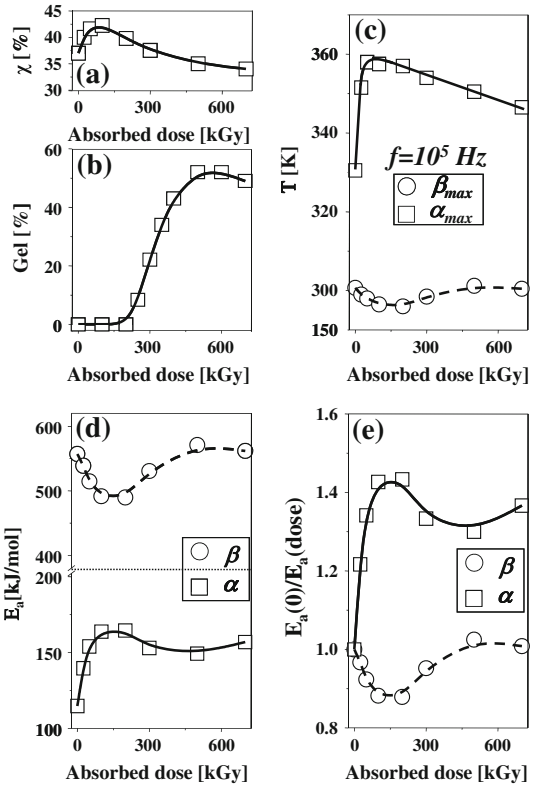

Fig. 3 **a** Crystallinity, **b** gel content versus absorbed dose; **c** dielectric relaxation loss maxima and **d** apparent activation energy (E_a) for the dielectric α and β processes versus absorbed dose; **e** E_a (dose)/E_a (0) ratio versus absorbed dose, where E_a (0) and E_a (dose) are apparent activation energies of the virgin and irradiated iPP, respectively

the fact that the oxygen present in the bulk and consumed due to radiation-induced reactions is not supplied fast enough by diffusion at higher doses. Apparently, the radiation-induced oxidation is limited by insufficient diffusion rate of oxygen and the accessibility of free radicals to atmospheric oxygen [60]. Post-irradiation annealing also plays a significant role and contributes to the saturation in carbonyl and hydroperoxide contents. Annealing at elevated temperatures introduces a much higher rate of thermal recombination of free radicals than the rate of oxygen diffusion from the surface into the film; this effect is more pronounced for the higher absorbed doses, i.e. for the higher concentrations of free radicals and in the samples with higher crystallinity, since the free radicals trapped in the crystalline area are the main cause of the post-irradiation oxidation observed in the case of gamma-irradiated PP [54].

On the basis of a comparison of IR spectroscopic and dielectric measurements, similar radiation-induced evolution in the concentration of carbonyl groups (Fig. 2b) and in the intensity (dielectric loss tangent maxima) of the β and α relaxations is observed (Fig. 2c, d). This is expected since the intensity of the dielectric relaxations in irradiated iPP depends over and above other parameters on the number of polar groups formed as a result of oxidation. The deviation in the intensity of the dielectric α and β relaxations from linear dependence is even more

emphasised at higher absorbed doses than in the case of carbonyl content (Fig. 2). It is necessary to bear in mind that in the case of dielectric losses there is a contribution not only from carbonyl but also from other polar (mainly hydroperoxide) groups connected with the specific relaxation and the phase in which the relaxation occurs. Thus, the larger deviation from the linear dependence in the intensity of the dielectric α and β relaxations than in carbonyl content can probably be explained by additional contribution of hydroperoxides; the concentration of hydroperoxides first increases for low-absorbed doses ($\leq$100 kGy) and then levels off for median doses and starts decaying with further increase in the radiation dose [6]. Furthermore, at higher irradiation doses, cross-linking suppresses chemicrystallization that originates from the morphological rearrangement of polymer fragments after chain scission events (Fig. 3a). Thus, the deviation of the relaxation intensity from the linear dependence is even more emphasised for the dielectric α process (Fig. 2d). Because of the nature of the α relaxation and since the fact that this relaxation shows larger increase with absorbed dose than the β relaxation at the same frequency (Fig. 1), it can be concluded that oxidative degradation occurs primarily on boundary layers between the amorphous and crystalline phase.

Crystallinity as a function of radiation dose is presented in Fig. 3a. A little increase in crystallinity is evident for low-radiation doses and is followed by a decrease for higher doses ($\geq$100 kGy). In many studies, the increase in crystallinity has been attributed to lamellar thickening and/or the increase in crystal perfection or to the formation of new lamellae by chemicrystallization of small fractions produced by chain scission during irradiation [61, 62]. On the other hand, the decrease in crystallinity was attributed to the formation of cross-linking [63] and to the radiation-induced defects within the crystals, as well as to those at the lateral grain boundaries [26, 32]. The decrease in crystallinity is concomitant with the increase in the gel content observed in Fig. 3b. It can be noticed that iPP undergoes scission for the absorbed doses $D < 200$ kGy. Irradiation of iPP with higher doses, due to more intense cross-linking behaviour, leads to a significant gel formation (three-dimensional network). In general, many studies indicate that in the absence of an effective cross-linking co-agent and/or acetylene as a cross-linking medium much higher doses ($\geq$250 kGy) are required before the dose to incipient gelation is reached and the effects of significant levels of cross-linking begin to show [30, 31, 64–66]. The maximum cross-linking of iPP irradiated in air takes place at a dose of 500 kGy. Irradiation for higher doses ($D > 500$ kGy) leads to saturation and even to a small decay in the gel content. The estimated values from the C–P equation ($D_G = 214$ kGy, $G(S) = 0.362$, $G(X) = 0.257$, $G(S)/G(X) = 1.41$, $g_{max} = 77.2$ and $f_c = 0.963$) are in good agreement with the literature data [21]. Herein, the dose required to reach the gel point is the gelation dose (D_G), $G(S)$ and $G(X)$ are radiation yields of scission and cross-linking, g_{max} is the calculated gel fraction for infinite dose and f_c is the correlation coefficient of linear regression.

Besides the changes in the relaxation intensity, radiation also induces changes in the distribution of relaxation times, peak position and activation energy of dielectric relaxations. Different origin/nature of the dielectric α and β relaxations leads to different evolutions with gamma radiation. The variations in the position and apparent activation energy of the dielectric α and β relaxations with absorbed

dose are shown in Fig. 3c, d, respectively. Additional changes in the glass-transition temperature T_g and the dynamic fragility m with absorbed dose are presented in Table 1. The position of the dielectric β relaxation is slightly shifted to lower temperatures at low-irradiation doses ($\leq$200 kGy); this shift together with the decrease in the apparent activation energy and the dynamic fragility can be attributed to the domination of chain scission reactions. For higher doses at which the cross-linking reactions become dominant (Fig. 3b), a recovery of temperature, dynamic fragility and the apparent activation energy for this relaxation is more than evident (Table 1; Fig. 3c, d). Contrary to this, the explanation for the large radiation-induced shift in the position and increase in activation energy of the dielectric α relaxation is not so simple. This shift is most intensive for lower doses ($\leq$100 kGy) at which the gel content is zero and oxidative degradation dominates. Thus, it is not possible to make the correlation between the shift in the position of the dielectric α relaxation and the cross-linking. Furthermore, WAXD data have indicated that the radiation-induced changes in crystallinity and crystal size can have some but not decisive influence on the position of the α relaxation. The crystallinity and crystal size for highly irradiated samples are smaller than those for the unirradiated one (Fig. 3a) [6], but the dielectric α relaxation still occurs at much higher temperatures (Fig. 3c). The most probable explanation for the observed shift with radiation is connected with the complex and multiple nature of this relaxation. A study of multiple dielectric α peaks in experimental spectra of virgin, annealed and irradiated iPP samples is presented in our previous paper [6]. The low-temperature component (α_1) is dominant in the unirradiated samples, while for the irradiated ones high-temperature components are prevalent, especially at lower doses. With further increase in absorbed dose, the decay in the position of the dielectric α relaxation can be explained by partial recovery of the low-temperature component (α_1), probably due to the intensive cross-linking behaviour. Thus, the shift in the position of the dielectric α relaxation can presumably be explained by the prevalence of high-temperature components (α_2 and α_3) in this relaxation due to the radiation-induced oxidative degradation. The reason for a more intensive increase in the high-temperature component with absorbed dose is difficult to nominate, but it is well known that each relaxation component can have a different sensibility to the oxidative degradation and introduction of specific polar groups, as well as to the cross-linking and net formation. The changes in activation energies with absorbed dose are relatively similar to those observed for the position of the dielectric α relaxation (Fig. 3c, d). The ratio of the activation energy of the irradiated samples E_a (dose) to the activation energy of the unirradiated one E_a (0), E_a (dose)/E_a (0), shows the degree of relative changes in the dielectric α and β relaxations due to gamma radiation (Fig. 3e). It is evident that the effect of ionizing radiation on the activation energy is more emphasised for the dielectric α relaxation. All the data presented indicate that the radiation-induced changes in the intensity, distribution of relaxation times, peak position and activation energy of the dielectric α relaxation are mach larger than in the case of the dielectric β relaxation, e.g. glass transition.

Conclusions

DRS and gamma radiation were used as powerful methods for characterization and modification of iPP, respectively. The disappearance of the low-temperature dielectric (δ and γ) relaxations with gamma radiation is connected with a large radiation-induced oxidative degradation. The radiation-induced increase in the amount of polar (mainly carbonyl and hydroperoxide) groups in apolar iPP causes an increase in polarity, and thus the increase observed in the magnitude of the dielectric α and β processes can clearly be connected with the radiation-induced oxidation, too. Because of the nature of the dielectric α relaxation and the fact that this relaxation shows larger increase with absorbed dose than the β relaxation, it can be concluded that oxidative degradation occurs primarily on boundary layers between the amorphous and crystalline phase. Besides the changes in the relaxation intensity, radiation also induces changes in the distribution of relaxation times, peak position and activation energy of the dielectric α and β relaxations. Variations in the position, dynamic fragility and apparent activation energy of the dielectric β relaxation are observed with radiation dose and can be connected with chain scission and cross-linking events. The decrease in the peak position (temperature), glass-transition temperature, dynamic fragility and apparent activation energy at lower radiation doses ($\leq$200 kGy) can be attributed to domination of chain scission reactions. At higher doses at which the cross-linking reactions predominate, the recovery in temperature, dynamic fragility and the apparent activation energy is clearly evident. Contrary to this, the explanation for the changes in the position and activation energy of the dielectric α relaxation is not so simple. The increase in the peak position (temperature) and activation energy is most intensive for lower doses ($\leq$100 kGy) at which the gel content is zero and oxidative degradation dominates. Thus, it is not possible to make a correlation between the shift in the position of the dielectric α relaxation and the cross-linking. On the other hand, radiation-induced changes in crystalline phase have some influence on the position and activation energy of the dielectric α relaxation, but the observed behaviour of this relaxation cannot be explained only by this. The crystallinity and crystal size for highly irradiated samples are smaller than those for the unirradiated one, but the dielectric α relaxation still occurs at much higher temperatures. The most probable explanation for the observed shift with radiation is connected with the complex and multiple nature of this relaxation; it can be found in the prevalence of high-temperature relaxation processes probably characterized by higher activation energies. Deviation from such behaviour is evident at higher doses at which cross-linking dominates over the oxidative degradation and a significant level of net formation is achieved. However, all the data presented here indicate that the radiation-induced changes in the intensity, distribution of relaxation times, peak position and activation energy of the dielectric α relaxation are larger than in the case of the dielectric β relaxation, e.g. glass transition. Great sensitivity of iPP structure to radiation-induced oxidative degradation and uncommon evolution in the dielectric δ, γ and α relaxation zones with high-energy radiation should be pointed out as the main conclusion.

Acknowledgment This study has been supported by the Ministry of Education and Science of the Republic of Serbia (Grant No. 172026).

References

1. Zhuravlev SP, Zhuravleva NM, Polonskij YuA (2002) Deformation characteristics of polypropylene film and thermal stability of capacitor insulation made on the base of polypropylene film. Elektrotekhnika 11:36–40
2. Fournie R (1990) All film power capacitors. Endurance tests and degradation mechanisms. Bulletin de la Direction des etudes et recherches Serie B 1:1–31
3. Montanari GC, Fabiani D, Palmieri F, Kaempfer D, Thomann R, Mülhaupt R (2004) Modification of electrical properties and performance of EVA and PP insulation through nanostructure by organophilic silicates. IEEE Trans Dielectr Electr Insul 11(5):754–762
4. Umemura T, Suzuki T, Kashiwazaki T (1982) Impurity effect of the dielectric properties of isotactic polypropylene. IEEE Trans Electr Insul EI-17(4):300–305
5. Fouracre RA, MacGregor SJ, Judd M, Banford HM (1999) Condition monitoring of irradiated polymeric cables. Radiat Phys Chem 54(2):209–211
6. Suljovrujic E, Trifunovic S, Milicevic D (2010) The influence of gamma radiation on the dielectric relaxation behaviour of isotactic polypropylene. The α relaxation. Polym Degrad Stab 95:164–171
7. Jourdan C, Cavaille JY, Perez J (1989) Mechanical relaxations in polypropylene. A new experimental and theoretical approach. J Polym Sci B 27(11):2361–2384
8. Brandrup J, Immergut EH (1975) Polymer handbook. Wiley, New York
9. Gitsas A, Floudas G (2008) Pressure dependence of the glass transition in atactic and isotactic polypropylene. Macromolecules 41(23):9423–9429
10. Starkweather HW, Avakian P, Matheson RR, Fontanella JJ, Wintersgill MC (1992) Ultralow temperature dielectric relaxations in polyolefins. Macromolecules 25(25):6871–6875
11. Quijada-Garrido I, Barrales-Rienda JM, Pereña JM, Frutos G (1997) Dynamic mechanical and dielectric behavior of erucamide (13-*cis*-docosenamide), isotactic poly(propylene), and their blends. J Polym Sci B 35(10):1473–1482
12. Sakai A, Tanaka K, Fujii Y, Nagamura T, Kajiyama T (2005) Structure and thermal molecular motion at surface of semi-crystalline isotactic polypropylene films. Polymer 46:429–437
13. Castejón ML, Tiemblo P, Gómez-Elvira JM (2001) Photo-oxidation of thick isotactic polypropylene films. II. Evolution of the low temperature relaxations and of the melting endotherm along the kinetic stages. Polym Degrad Stab 71(1):99–111
14. Perepechko II (1977) Svoistva polimerov pri nizkih temperaturah. Khimiya, Moskva
15. Hara T (1967) Dielectric property of some polymers in low temperature region. Jpn J Appl Phys 6:147–150
16. Hoyos M, Tiemblo P, Gómez-Elvira JM (2007) The role of microstructure, molar mass and morphology on local relaxations in isotactic polypropylene. The α relaxation. Polymer 48(1):183–194
17. Tiemblo P, Gomez-Elvira JM, García Beltrán S, Matisova-Rychla L, Rychly J (2002) Melting and α relaxation effects on the kinetics of polypropylene thermooxidation in the range 80–170 °C. Macromolecules 35(15):5922–5926
18. Pluta M, Kryszewski M (1987) Studies of alpha-relaxation process in spherulitic and non-spherulitic samples of isotactic polypropylene with different molecular ordering. Acta Polym 38(1):42–52
19. Banford HM, Fouracre RA, Faucitano A, Buttafava A, Martinotti F (1996) The influence of chemical structure on the dielectric behavior of polypropylene. IEEE Trans Dielectr Electr Insul 3(4):594–598
20. Olivares N, Tiemblo P, Gomez-Elvira JM (1999) Physicochemical processes along the early stages of the thermal degradation of isotactic polypropylene I. Evolution of the γ relaxation under oxidative conditions. Polym Degrad Stab 65(2):297–302
21. Suljovrujic E (2009) Gel production, oxidative degradation and dielectric properties of isotactic polypropylene irradiated under various atmospheres. Polym Degrad Stab 94:521–526
22. Arranz-Andrés J, Peña B, Benavente R, Pérez E, Cerrada ML (2007) Influence of isotacticity and molecular weight on the properties of metallocenic isotactic polypropylene. Eur Polym J 43(6):2357–2370
23. McCrum NG (1964) Density-independent relaxations in polypropylene. J Polym Sci B 2(5):495–498
24. Read BE (1990) Mechanical relaxation in isotactic polypropylene. Polymer 30(8):1439–1445

25. Ribes-Greus A, Diaz-Calleja R (1989) Dielectric relaxations of high and low density irradiated polyethylene. J Appl Polym Sci 38(6):1127–1143
26. Chodak I (1995) Properties of crosslinked polyolefin-based materials. Prog Polym Sci 20(6): 1165–1199
27. Chapiro A (1962) Radiation chemistry of polymeric systems (high polymers S.). Interscience Publishers, Wiley, New York, London
28. Singh A, Silverman J (eds) (1991) Radiation processing of polymers. Hanser Publishers, Munich
29. Dole M (1972) The radiation chemistry of macromolecules, vol 1. Academic Press, New York, London
30. Dole M (1973) The radiation chemistry of macromolecules, vol 2. Academic Press, New York
31. Mark EJ (1996) Physical properties of polymers handbook. American Institute of Physics, Woodbury
32. Suljovrujic E (2009) The influence of molecular orientation on the crosslinking/oxidative behaviour of iPP exposed to gamma radiation. Eur Polym J 45(7):2068–2078
33. Abdel-Hamid HM (2005) Effect of electron beam irradiation on polypropylene films—dielectric and FT-IR studies. Solid State Electron 49(7):1163–1167
34. Banford HM, Fouracre RA, Faucitano A, Buttafava A, Martinotti F (1996) The influence of γ-irradiation and chemical structure on the dielectric properties of PP. Radiat Phys Chem 48:129–130
35. Dadbin S, Frounchi M, Saeid MH, Gangi F (2002) Molecular structure and physical properties of e-beam crosslinked low-density polyethylene for wire and cable insulation applications. J Appl Polym Sci 86:1959–1969
36. Suljovrujic E (2005) Some aspects of structural electrophysics of irradiated polyethylenes. Polymer 46(17):6353–6359
37. Myśliński P, Kryszewski M (1980) The effect of spherulite structure of polypropylene on the thermally stimulated electret depolarization current. Polym Bull 2(11):761–768
38. Yamashita T, Ikezaki K (2005) A method for correlating charge traps of polypropylene to its morphology. J Electrost 63(6–10):559–564
39. Boyd RH (1985) Relaxation processes in crystalline polymers: experimental behavior—a review. Polymer 26(3):323–347
40. Mansfield M, Boyd RH (1978) Molecular motions, the α relaxation, and chain transport in polyethylene crystals. J Polym Sci 16(7):1227–1252
41. McCrum NG (1984) The kinetics of the α and β relaxations in isotactic polypropylene. Polymer 25(3):299–308
42. Kessairi K, Napolitano S, Capaccioli S, Rolla P, Wübbenhorst M (2007) Molecular dynamics of atactic poly(propylene) investigated by broadband dielectric spectroscopy. Macromolecules 40(6): 1786–1788
43. Qin Q, McKenna GB (2006) Correlation between dynamic fragility and glass transition temperature for different classes of glass forming liquids. J Non-Cryst Solids 352(28–29):2977–2985
44. Roy SK, Kyu T, Manley RStJ (1988) Physical and dynamic mechanical properties of ultradrawn polypropylene films. Macromolecules 21(2):499–504
45. Razavi-Nouri M (2005) Thermal and dynamic mechanical properties of a polypropylene random copolymer. Iran Polym J (English Edition) 14(5):485–493
46. Frubing P, Blischke D, Gerhard-Multhaupt R, Salah Khalil M (2001) Complete relaxation map of polyethylene: filler-induced chemical modifications as dielectric probes. J Phys D Appl Phys 34(20):3051–3057
47. Plazek D, Ngai KL (1991) Correlation of polymer segmental chain dynamics with temperature-dependent time-scale shifts. Macromolecules 24(5):1222–1224
48. Banford HM, Fouracre RA, Chen G, Tedford DJ (1992) Electrical conduction in irradiated low-density polyethylene. Radiat Phys Chem 40(5):401–410
49. Hedvig P (1977) Dielectric spectroscopy of polymers. Academia Kiado, Budapest
50. Magerramov AM, Dashdamirov MK (2005) Structural aspects of the radiation modification of the dielectric properties of polyolefins. High Energy Chem 39(3):142–147
51. Fouracre RA, Banford HM, Given MJ (1993) Charge migration processes in insulators. High Temp Chem Process 2:257–264
52. Lu T, Sessler GM (1991) An experimental study of charge distributions in electron-beam irradiated polypropylene films. IEEE Trans Electr Insul 26(2):228–235
53. Vannikov AV, Matveev VK, Sichkar VP, Tutnev AP (1982) Radiacionnie effekti v polimerah. Elektricheskie svoistva. Izdatel'stvo Nauka, Moskva

54. Rivaton A, Lalande D, Gardette J-L (2004) Influence of the structure on the γ-irradiation of polypropylene and on the post-irradiation effects. Nucl Instrum Methods Phys Res B 222:187–200
55. Bertoldo M, Bronco S, Cappelli C, Gragnoli T, Andreotti L (2003) Combining theory and experiment to study the photooxidation of polyethylene and polypropylene. J Phys Chem B 107(11880):11888
56. Krause B, Haußler L, Voigt D (2006) Comparison of the molecular properties and morphology of polypropylenes irradiated under different atmospheres and after annealing. J Appl Polym Sci 100(1):634–639
57. Lacoste J, Vaillant D, Carlsson DJ (1993) Gamma-, photo-, and thermally-initiated oxidation of isotactic polypropylene. J Polym Sci A 31(3):715–722
58. Lacoste J, Vaillant D, Chmela S (1996) Gamma-, photo- and thermally-initiated oxidation of polyolefines used in packaging. J Polym Eng 15(1–2):139–152
59. Gavrila DE, Gosse B (1994) Post-irradiation degradation of polypropylene. J Radioanal Nucl Chem 185(2):311–317
60. Shinde A, Salovey R (1985) Irradiation of ultrahigh-molecular-weight polyethylene. J Polym Sci 23(8):1681–1689
61. Alariqi SAS, Kumar AP, Rao BSM, Singh RP (2009) Effect of γ-dose rate on crystallinity and morphological changes of γ-sterilized biomedical polypropylene. Polym Degrad Stab 94(2):272–277
62. Suljovrujic E (2000) Radiation modification of the physical properties of polyolefins. University of Belgrade, Belgrade
63. Stojanovic Z, Kacarevic-Popovic Z, Galovic S, Milicevic D, Suljovrujic E (2005) Crystallinity changes and melting behavior of the uniaxially oriented iPP exposed to high doses of gamma radiation. Polym Degrad Stab 87(2):279–286
64. Krause B, Voigt D, Haußler L, Auhl D, Münstedt H (2006) Characterization of electron beam irradiated polypropylene: influence of irradiation temperature on molecular and rheological properties. J Appl Polym Sci 100(4):2770–2780
65. Lugao AB, Cardoso ECL, Lima LFCP, Hustzler B, Tokumoto S (2003) Characterization study of gamma-irradiated, high melt-strength polypropylene. Nucl Instrum Methods Phys Res B 208(1–4): 252–255
66. Jones RA, Cail JI, Stepto RFT, Ward IM (2000) Atomistic and Flory–Stockmayer analyses of irradiated i-PP gel fractions and comparison with results from PE. Macromolecules 33(20): 7337–7344